Iranian Journal of Microbiology

*Volume 15 Number 1 (February 2023) 138-148*

ORIGINAL ARTICLE

# Antiviral activity of biosynthesized copper nanoparticle by *Juglans regia* green husk aqueous extract and Iron nanoparticle: molecular docking and *in-vitro* studies

**Mahsa Ahmadi[1], Ameneh Elikaei[1*], Parinaz Ghadam[2]**

*[1]Department of Microbiology, Faculty of Biological Sciences, Alzahra University, Tehran, Iran*
*[2]Department of Biotechnology, Faculty of Biological Sciences, Alzahra University, Tehran, Iran*

**Received:** June 2022**, Accepted:** January 2023

## ABSTRACT

**Background and Objectives:** The interaction between nanoparticles (NPs) and viruses is attracting interest because of the antiviral potential of NPs. This study aims to investigate the antiviral potential of NPs against Herpes simplex virus types 1 (HSV-1).

**Materials and Methods:** Molecular docking studies were conducted by Molegro virtual docker software. An extract of *Juglans regia* green husk was utilized to biosynthesize copper-oxide nanoparticles (CuNPs). The cytotoxicity of NPs was evaluated by MTT assay. Different treatment assays were conducted. Another assay was designed to employ the concentration of 300 µg/ml of CuNPs, which is the highest concentration that did not precipitate. Finally, chemically synthesized Iron oxide nanoparticles (FeNPs) were utilized to adsorb CuNPs. The antiviral effect of FeNPs was investigated, separately.

**Results:** Docking results confirmed that NPs could interact with the HSV-1 glycoproteins and prevent viral entry. MTT assay results illustrated that the minimum non-toxic concentration (MNTD) of CuNPs is 100 µg/ml which did not exhibit antiviral properties. Employing a noncytotoxic concentration of FeNPs (300 mg/ml) in combination with cytotoxic concentration of CuNPs (300 µg /ml), eliminated the cytotoxicity effects of CuNPs. Exposure of the virus with the combination of CuNPs and FeNPs resulted in 4.5 log10 $TCID_{50}$ reductions in HSV-1. While treating HSV-1 with only FeNPs reduced the titer of virus by 3.25 log10 $TCID_{50}$.

**Conclusion:** The results highlight that combination of CuNPs and FeNPs have antiviral activity against HSV-1. Moreover, FeNPs demonstrated antiviral properties against HSV-1 separately.

**Keywords:** Antiviral; Herpes simplex virus types 1; Copper-oxide; Iron oxide; Nanoparticles

## INTRODUCTION

The world population faces the problem of viral infection and the various life-threatening diseases caused by different viruses. Emerging and re-emerging viral infections are causing epidemic outbreaks in human societies. Although tremendous improvement has been made from time to time in the field of antiviral therapy, medicines are unable to completely prevent all viral diseases. Furthermore, the choice for antivirals against viral diseases is currently very limited and the emergence of drug-resistant strains is frequently encountered (1). Therefore, there is an urgent need to find new and potentially useful mole-

*Corresponding author: Ameneh Elikaei, Ph.D, Department of Microbiology, Faculty of Biological Sciences, Alzahra University, Tehran, Iran. Tel: +98-21-85692726 Fax: +98-21-88058912 Email: a.elikaei@alzahra.ac.ir

cules for the prevention and therapies of viral diseases. The design of disease-specific nanomedicines is feasible at present as an alternative to counter such traits. Recently, nano-structured metallates were studied for preferential attachment with the virion surface, cell entry inhibition, and early containment of viral infections (2). Herpes simplex virus types 1 (HSV-1) is an important virus because it can cause serious infections in humans.

HSV-1 is an enveloped and double-stranded DNA virus belonging to the *Herpesviridae* family and *Alphaherpesvirinae* subfamily (3). HSV-1 is surrounded by an icosahedral capsid which is encased by a bilayer lipid envelope containing different viral glycoproteins including glycoprotein D (gD), glycoprotein B (gB), and glycoprotein H/L(gH/gL). HSV-1 is one of the most prevalent pathogens that are often acquired during childhood and remain latent in the nervous system (4). HSV-1 is a neurotropic pathogen with a wide diversity of clinical manifestations ranging from harmless skin infections such as ulcerative and vesicular oral/facial lesions to harmful central nervous system infections. In adults, the serious clinical outcomes of HSV-1 vary from encephalitis with long-term consequences to herpetic keratitis leading to blindness (5). Acyclovir (ACV) also known as acycloguanosine was discovered in 1977-1978, and after more than 40 years, ACV and its pro-drugs are still current therapeutic options against HSV-1 infections and reactivation (6). However, ACV has several limitations including low absorption and bioavailability (15-20%), the short elimination half-life of 2.5-3 hours post-administration requiring frequent and high drug usage, and side effects (7). Besides, the drug-resistant strains of HSV-1 emerge among high-risk groups such as patients with immunocompromised status and patients who had transplantation (8). Hence, the development of safer and more effective alternatives to treat HSV-1 appears crucial.

Nanotechnology provides new methods in the era of medicine. Nanoparticles (NPs) are a wide class of materials that have attracted great attention because of their specific physical and chemical properties, including smaller sizes (1-100 nanometers), a higher quantity of surface atoms, and high surface-to-volume ratios. Therefore, they have shown potential applications in drug designing and diagnostic medicine (9). To date, many metal NPs have been widely studied for their anti-microbial properties against a wide spectrum of human pathogens, including parasites, fungi, bacteria, and viruses. Copper oxide nanoparticles (CuNPs) and Iron nanoparticles (FeNPs) have shown wide commercial applications in industry, as well as potential physical properties and their cheap production cost. Several studies have investigated the inhibitory effects of them against viruses; however, most researchers have focused on antibacterial properties (10).

Various methods are applied to synthesize NPs including physical, chemical, and biological methods, and each of these approaches has several advantages and drawbacks (11). The biological synthesis method employs biological systems such as aqueous plant extracts, bacteria, fungi, viruses, yeast, and actinomycetes for the synthesis of NPs. In these cases, producing agents or other constituents present in the cells act as stabilizing and capping agents; thus, there is no need to add capping and stabilizing agents from the outside (12). While the chemical synthesis of NPs is a two-step process including the production and capping of the NPs (13).

In this study, molecular docking studies were conducted to explore virus-NP interactions that might result in the NP's antiviral activities. Computational studies were followed by in-vitro experiments which could help to understand more about the cytotoxicity of synthesized CuNPs and FeNPs to the Vero cell line as well as their antiviral activity against HSV-1 *in-vitro* amplification.

## MATERIALS AND METHODS

**Molecular docking.** The unit cells of CuNPs and FeNPs were made according to the library of Materials Studio 2017 software. Using the steepest descent algorithm of Avogadro software, the final optimized and energy minimized the 3D structures of the NPs were generated. The PDB file of the 3D structure of HSV-1 gD (PDB ID: 2C3A), gB (PDB ID: 3NWF), and gL/gH (PDB ID: 3MIC) envelope glycoproteins were obtained from RCSB protein data center. The protein structure was minimized using the steepest descent minimization algorithm. In our study, viral proteins were considered as receptor and our synthetic NPs as ligands. Protein structures of viruses were prepared for docking studies by removal of water and ligands molecules, and docking study was conducted by Molegro virtual docker (MVD) software. Molegro Virtual Docker is a protein–ligand docking

simulation tool which determines the optimal geometry of flexible ligands in interaction with protein. The docking process was performed after determining the binding site in the protein and the binding mode in the ligand. Ten sets of docking were run followed by post-dock energy minimization by applying the Nelder-Mead Simplex Minimization. The outcomes were analyzed using Molegro Molecular Viewer 7.0 and the best interacting poses were selected.

**Biosynthesis of CuNPs by aqueous extract of *J. regia* green husk.** The 0.4 g of dried husk powder of *J. regia* was added to 14.5 mL of boiling distilled water in an Erlenmeyer flask. The flask was kept for 10 min in a Ben Murray. The aqueous extract was filtered by a piece of Whatman paper no. 1 (Catalogue Number: WHA-1001-90). The 0.018 g of copper acetate was added to 10 ml of water to obtain a 1 mM concentration. Ultimately, 1.5 ml of the extract was added to 10 mL of copper acetate solution and 90 ml of water. The sample was incubated in ambient conditions and darkness. After 24 h the sample was investigated for any color shift as an initial sign of CuNPs successful biosynthesis. Then, the sample was centrifuged (Hettich zentrigujen, ROTINA380R) at 4588.272 – 6245.148 × g for 30 min to remove the aqueous extract of *J. regia* green husk from the sample. The CuNPs pellet moved to another dry vial. CuNPs pellet was centrifuged (MiniSpin, Eppendorf, Hamburg, Germany) 2 times at 12045 ×g for 30 min to ensure all extract was removed from the sample. The pellet was dried in a heat block at 70°C (14). Then distilled water was added to the pellet in order to obtain a 300 µg/ml concentration of CuNPs which was stable for 24 h to conduct the MTT(3-(4,5-dimethylthiazol-2-yl)-2,5 diphenyltetrazolium bromide) assay test. The sample was sonicated 8 times, each time for 15 min at the frequency of 37 kilohertz (kHz) in an Ultrasonicator bath (Elmasonic S60, Germany) to achieve CuNPs colloid.

**Chemical synthesize of the FeNPs.** 6.95 g of $FeSO_4.7H_2O$ and 10 g of $Fe_2(SO_4)_3$ were added to 250 mL of distilled water. Ammonium hydroxide (25%) was dropped wisely to adjust the pH to 10. The sample was stirred and heated on a heater–stirrer plate at 60°C for 1 h. A 10 × 15 mm neodymium magnet was utilized to separate the FeNPs. Then, the water was added to the sample with pH 7. The sample was dried for 2 h at 60°C in a heat block (15).

**Cells and viral strains.** African green monkey kidney (Vero) cell line (NCBI No. C101) was obtained from Pasteur institute of Iran. Vero cell line were maintained in Dulbecco's Modified Eagle's Medium (DMEM) supplemented with 10% Fetal Bovine Serum (FBS). The cells were kept at 37°C in a humidified incubator in an atmosphere of 5% $CO_2$. Herpes simplex virus type 1 was generously donated by the Iranian Blood Transfusion Organization. Viruses were propagated in Vero cell line and stored in sterile cryovials at -70°C until further use.

**Determination of the maximal non-cytotoxic concentration.** MTT assay was conducted to evaluate the cytotoxicity effects of CuNPs on the cell line. MTT assay is based on the reduction of yellowish MTT reagent to insoluble and dark blue formazan by NAD(P)H-dependent oxidoreductase enzymes of viable and metabolically active cells. The Vero cell line was seeded in 96-well plates and was exposed to decreasing concentrations of biosynthesized CuNPs including 250, 200, 150, 100, 80, 50, 40, 30, 20, 10, 5, 2.5, and 1.25 µg/ml. The 96-well plate was incubated for 24 hours at 37°C in a humidified incubator with 5% $CO_2$. After gently aspirating the 100 µl of the medium, 100 µl of MTT solution was added to each well, and the cells were incubated for a further 4 hours at 37°C. The medium with MTT solution was removed completely, and the formazan crystals were dissolved by adding 100 µl of dimethyl sulfoxide (DMSO). The absorption values were measured at 570 nm using an ELISA reader. Vero cell line viability in each well is presented as a percentage of control cells.

**Evaluation of the antiviral activity of CuNPs.** For cotreatment, cell post-treatment, and virus pretreatment assay, CuNPs were dissolved in DMEM medium without serum and used at the concentrations of 100, 80, 50, and 10 µg/ml. inhibition of infectivity was calculated by the $TCID_{50}$ assay.

**Cotreatment assay.** 96 well plates were seeded with Vero cell line, after reaching 80% confluency, the medium was removed and wells were washed with sterile PBS. Then, 50 µl of virus ($10^6$ $TCID_{50}$/mL virus particles of HSV-1) and 100 µl various concentrations of CuNPs were added to 50 µl of DMEM. Cells infected with the virus alone served as virus control (virus + DMEM) and Vero cell line alone served as cell control. The plate was incubated for 24 hours at

37ºC in 5% $CO_2$. After 24 hours plate was examined microscopically for cytopathic effect (CPE).

**Cell post-treatment assay.** Vero cell line monolayers (96-well plates) were incubated with 50 µl of HSV-1 for 2, 6, and 8h at 37°C. After 2, 6, and 8 h incubation, 100 µl of CuNPs were added to the inoculum followed by further incubation for 24 hours at 37°C in a humidified incubator with 5% $CO_2$. After 24 hours plate was evaluated microscopically for CPE.

**Virus pretreatment assay.** HSV-1 was incubated in the presence of different concentrations of CuNPs for 1 and 2 hours at 37°C, then 200 µl of treated viruses with CuNPs were added to the cell monolayers. Plates were incubated for 24 hours at 37°C in a humidified incubator in an atmosphere of 5% $CO_2$ to investigate viral CPE.

**Antiviral activity of FeNPs and CuNPs.** HSV-1 was incubated with 300 µg/ml concentrations of CuNPs for 1 hour. Then, samples were poured on dried FeNPs to obtain the final 300 mg/ml concentration of FeNPs, and they were vortexed for 3 min. Samples were sonicated 2 times, each time for 15 min at the frequency of 37 kHz. Afterward, supernatants were transferred into glass jars and incubated for a further 1 hour at 25°C and 0.3958 ×g in a shaker incubator (WIS-20R, Daihan Scientific Co., Ltd., Korea). After incubation at room temperature for 15 min, samples were exposed to the external magnetic field that was provided by a neodymium magnet for 10 min to separate the FeNPs from the adsorbed biogenic CuNPs. Supernatants were drained and added to DMEM to make 10-fold dilutions. Viruses treated with FeNPs alone served as a control to investigate the antiviral potential of FeNPs. Supernatants, dilutions, and controls were added to the cell monolayers. The plate was incubated at 37°C for 24 hours, and the CPE effects were examined with a converted microscope.

## RESULTS

Results of the docking study suggested that HSV-1 inactivation might be caused by a direct interaction between NPs and viral glycoproteins, which are involved in the attachment of HSV-1 to the host cell that can inhibit viral attachment and entry.

The docking modeling studies were conducted by MVD and the docking results were listed in Table 1. Confirmations of docked CuNPs (Fig. 1) ligand with viral glycoproteins were analyzed in terms of Total Energy or MolDock Score values that were dominated by the negative energy values, insinuating that the interactions between HSV-1 particles and NPs were spontaneous.

**Table 1.** Resulted in parameters from involvement between CuNPs ligands and HSV-1 glycoproteins of MVD

| Receptor | Ligand | MolDock Score |
|---|---|---|
| gD | CuNPs | -38.8617 |
| gB | CuNPs | -83.2684 |
| gH/gL | CuNPs | -76.3696 |

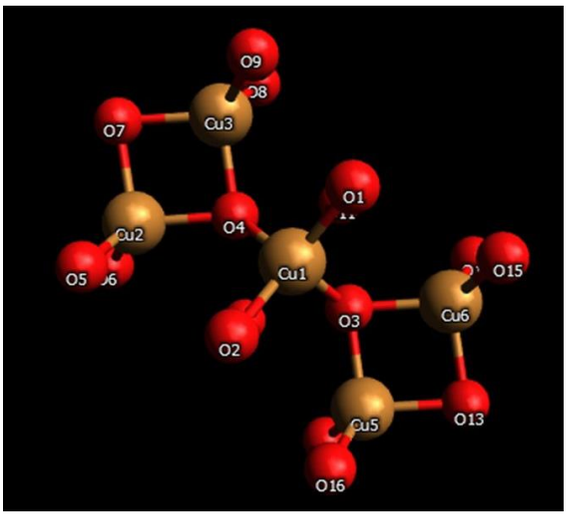


**Fig. 1.** Unit cell's molecular structure of CuNPs drawn by material studio software.

The data in Table 1 demonstrates that MolDock Scores of CuNPs interacted with gD, gB, and gH/gL glycoproteins were negative. The calculated minimum relative Free Total Energy values score implies that NPs reasonably interact with viral proteins. Hence, CuNPs could be effective against HSV-1 infections.

Fig. 2 shows the interaction of CuNPs ligands in the active site of HSV-1 glycoproteins. According to docking analysis data, CuNPs interactions with HSV-1 gD involved the formation of hydrogen bonds bounds with amino acids Gln 178, Thr 163, Tyr 59, Gly 103, and Pro 47, and steric interaction with amino acids Thr 163, Leu 165, Ile 180, Ile 55, and Met 102. The obtained data from docking analysis showed that

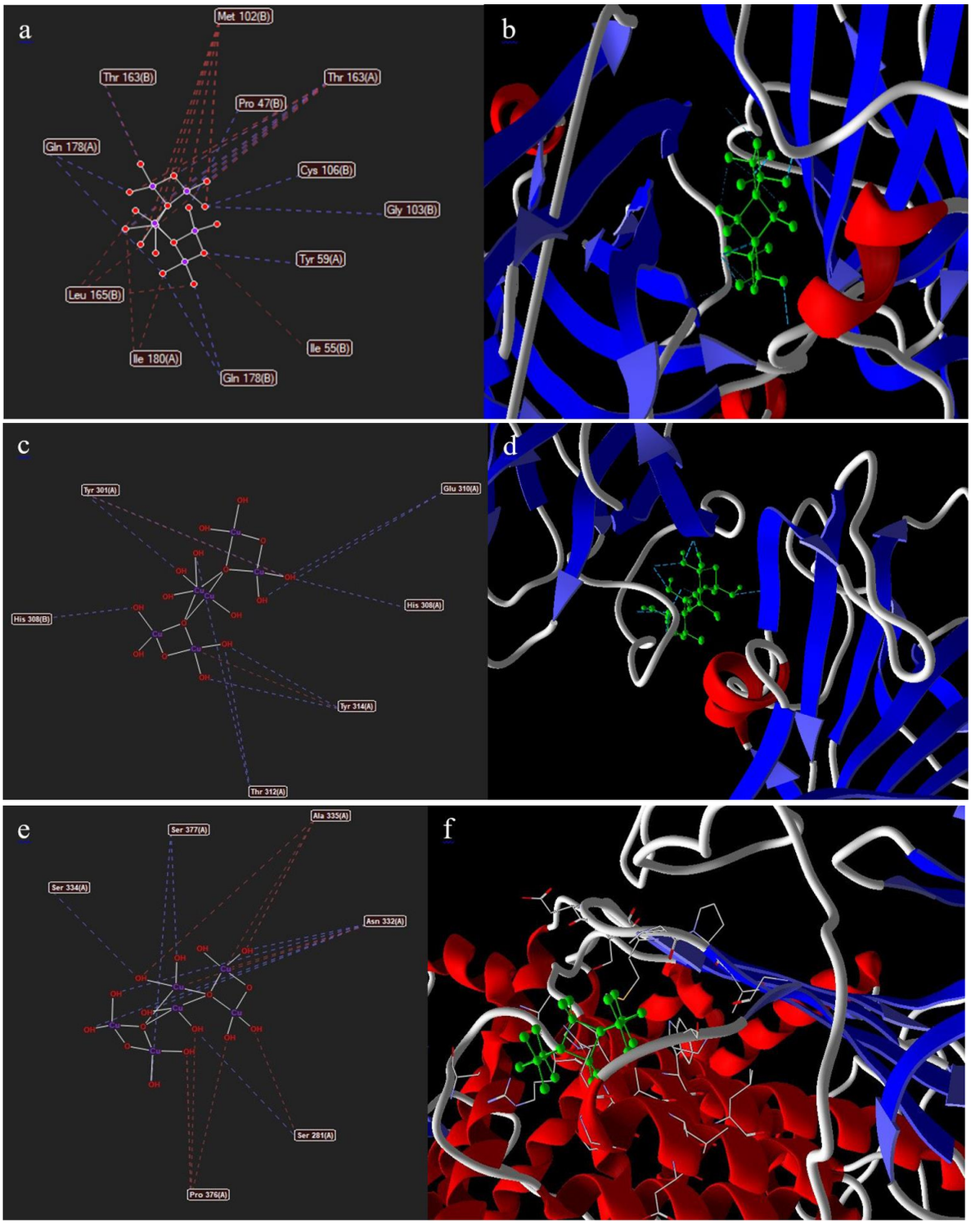


**Figs. 2.** a, b) The interactions between CuNPs and the amino acids of the HSV-1 gD. c, d) The interactions between CuNPs and the amino acids of the HSV-1 gB. e, f) The interactions between CuNPs and the amino acids of the HSV-1 gH/gL. Hydrogen bonds and steric interactions are shown as blue and red lines, respectively.

CuNPs form hydrogen bonds with HSV-1 gB amino acids Glu 310, His 308, Tyr 314, Thr 312, His 308, and Tyr 301, and make steric interaction with amino acids Tyr 301, and Tyr 314. Furthermore, the interactions of the CuNPs ligand with HSV-1 gH/gL glycoprotein include hydrogen bonds with amino acids Ser 334, Ser 377, Asn 332, and Ser 281, and steric interaction with amino acids Ala 335, Ser 281, and Pro 376.

The aqueous extract of *J. regia* green husk was treated with 1 mM copper acetate which resulted in changing the initial color of the sample to dark brown due to the conversion of $Cu^{2+}$ to CuNPs. This color shift is the early sign of the formation of CuNPs with an average size of 28 nm (14). The colloidal suspension displayed an SPR peak at 212 nm (16), which confirmed the formation of CuNPs (17) (Fig. 3).

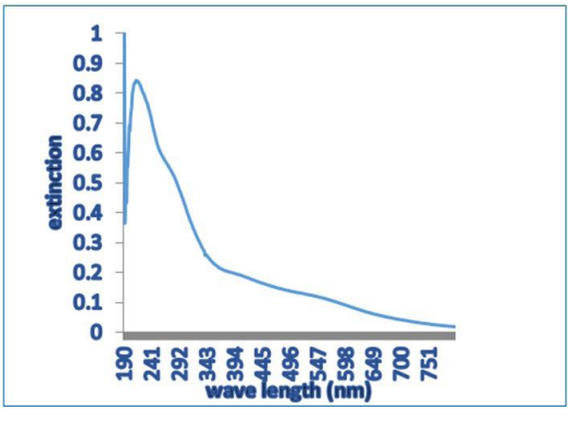


**Fig. 3.** The SPR peak of biosynthesized CuNPs

Since viruses proliferate only in host cells, it was essential to examine the toxicity of the CuNPs on the Vero cell line (18). Fig. 4 shows the percentage of viable cells after treatment by the NPs relative to control cultures. The cytotoxicity pattern revealed that CuNPs showed improved cell viability at a lower concentration. The results indicated that with the increase in the concentration of CuNPs to 200 µg/mL, the cell viability reduced to 20% compared to control cells. Also, there was a decrease in cell viability (22%) after the addition of CuNPs at the concentration of 150 µg/ml. Concentrations of 100 µg/ml exhibited a cytotoxic effect of less than 20% which was considered as minimum non-toxic dose (MNTD) and used for subsequent antiviral assays. Furthermore, when the combination of FeNPs and CuNPs was used, the higher concentration of CuNPs (300 µg/ml) and concentration of 300 mg/ml of FeNPs showed no cytotoxicity effects on the Vero cell line.

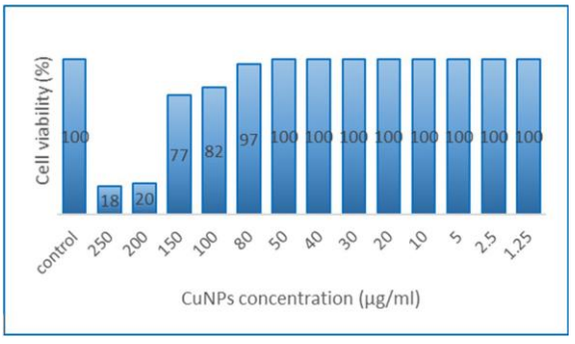


**Fig. 4.** Cytotoxicity of CuNPs on Vero cell line.

The results of the cotreatment assay, cell post-treatment assay, and virus pretreatment assay demonstrated that none of the noncytotoxic concentrations of CuNPs are efficient in reducing HSV-1 *in-vitro* amplification. Indeed, noncytotoxic concentrations of CuNPs did not exhibit antiviral properties against HSV-1 infections. Therefore, the other assay was designed to employ the concentration of 300 µg/ml of CuNPs, which is the highest concentration that did not precipitate during the reaction time (24 hours) and is stable. Considering the issue that concentrations of 300 µg /ml of CuNPs had cytotoxicity effects on Vero cell line, in this assay FeNPs were utilized to adsorb free CuNPs and subsequently reduced cell cytotoxicity to the acceptance level. Based on the study of Ayadi et al. the CuNPs were trapped onto the FeNPs with considerable efficiency (80%) (15). In addition, the antiviral effect of FeNPs against HSV-1 was investigated, separately.

The antiviral efficacy of the combination of CuNPs and FeNPs against HSV-1 was estimated by investigating the reduction of CPE and virus titer. Antiviral assay findings have shown that pre-treatment of HSV-1 with the combination of CuNPs and FeNPs (the concentration of 300 µg/ml CuNPs and 300 mg/ml of FeNPs) resulted in 4.5 log10 $TCID_{50}$ reduction in virus titers as compared with the virus control (VC) group. While 3.25 log10 $TCID_{50}$ reduction in virus titers was observed when HSV-1 was only treated with 300 mg/ml FeNPs (Fig. 5). The results revealed that the log10 $TCID_{50}$ reduction in HSV-1 titer due to treatment with the combination of CuNPs and FeNPs was greater than the log reduction due to treatment with only FeNPs. Consequently, combination of CuNPs and FeNPs demonstrated antiviral activity and reduced titer of viruses under the synergism mechanism, significantly.

The outcome of the docking studies of FeNPs (Fig. 6) with the HSV-1 glycoproteins is presented in Table 2, and Fig. 7. Negative energy values of docking stud-

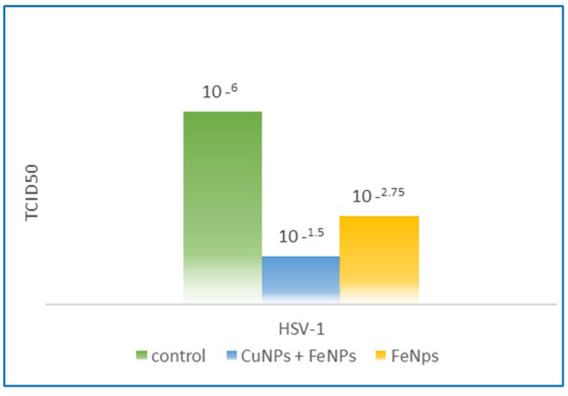


**Fig. 5.** Effect of CuNPs, FeNPs, and CuNPs on the titer of HSV-1 by 50% tissue culture infectious dose assay ($TCID_{50}$) in virus pre-treatment assay.

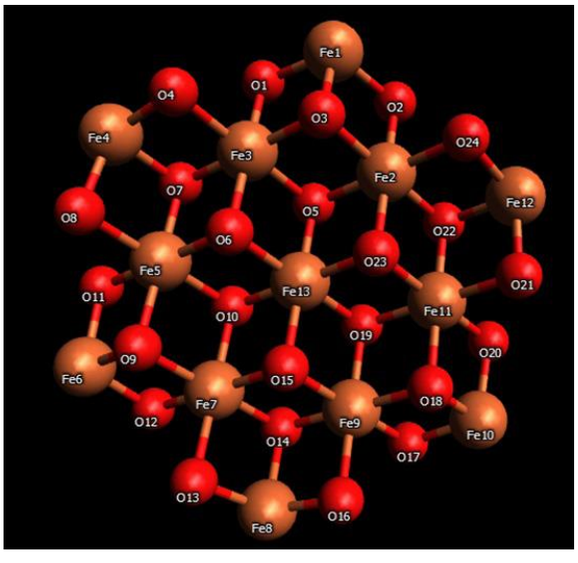


**Fig. 6.** Unit cell's molecular structure of FeNPs drawn by material studio software.

ies, confirm that the interactions between viral particles and FeNPs were spontaneous.

According to docking analysis data, FeNPs interactions with gD include hydrogen bonds with amino acids Tyr 59, Asn 105, Thr 163, and Gln 178, and steric bonds with Gln 178, Leu 165, Ile 180, Met 102, Phe 48, Gly 162, Gly 103, Gly 104, Asn 105, and Thr 163. FeNPs interactions with gB include hydrogen bonds with Tyr 301, and Thr 312 and steric bonds with Tyr 314, Ala 316, and Thr 312. Moreover, FeNPs form hydrogen bonds with HSV-1 gH/gL amino acids Ser 334, Ser 337, Ser 370, Ser 281, and Asn 332 and steric interactions with amino acids Ser 334, Ser 337, Pro 376, Ala 374, Asp 280, and Asn 332 (Fig. 7).

**Table 2.** Resulted in parameters from involvement between FeNPs ligands and HSV-1 glycoproteins of MVD.

| Receptor | Ligand | MolDock Score |
|---|---|---|
| gD gB | FeNPs | -78.6238 |
| gH/gL | FeNPs | -152.584 |
| | FeNPs | -143.673 |

## DISCUSSION

Antimicrobial activities of NPs against viruses, Gram-positive, and Gram-negative bacteria have been reported in previous studies (18). The process of adhesion and electrostatic interaction with the bacterial cell wall leads to disruption of the bacterial membrane integrity and ultimately leads to the death of microorganisms. Furthermore, NPs have the potential of neutralizing infectious viruses, including single/double-stranded DNA and RNA viruses such as bronchitis virus, poliovirus, and human immunodeficiency virus type-1. These NPs interact with viral proteins which this interaction may inactivate viral infection (19). This study aimed to investigate the antiviral potential of NPs to design materials containing these NPs to inhibit HSV-1 infections.

Plants extracts contain diverse groups of bioactive natural compounds such as; polysaccharides, proteins, pigments, and antioxidants that are biocompatible reductants. This enables the use of algae as a safe bio-friendly platform for metallic nanoparticle production (20). During this study, CuNPs were successfully synthesized in *J. regia* green husk. Initially, CuNPs was confirmed by color converted from yellowish to brown color, 24 hours of cultivation at room temperature. The brown color of the CuNPs is due to the Surface Plasmon Resonance (SPR) of these NPs, which is because of the interaction of the electrons of the conduction band with incident photons. The SPR is very sensitive to the size and shape of the particles, their inter particle distances, the surrounding media, and the environment (21).

NPs that could interact with the HSV-1 glycoproteins including gD, gB, and gH/gL, were hypothesized to interfere with virus attachment to host receptors and subsequently inhibit viral infection. These interactions might result in irreversible changes to the virus structure and a reduction of infection (22). HSV-1 capsid is encased by a bilayer lipid envelope containing ≥12 different viral proteins. Some of these proteins interact with host cell surface receptors and

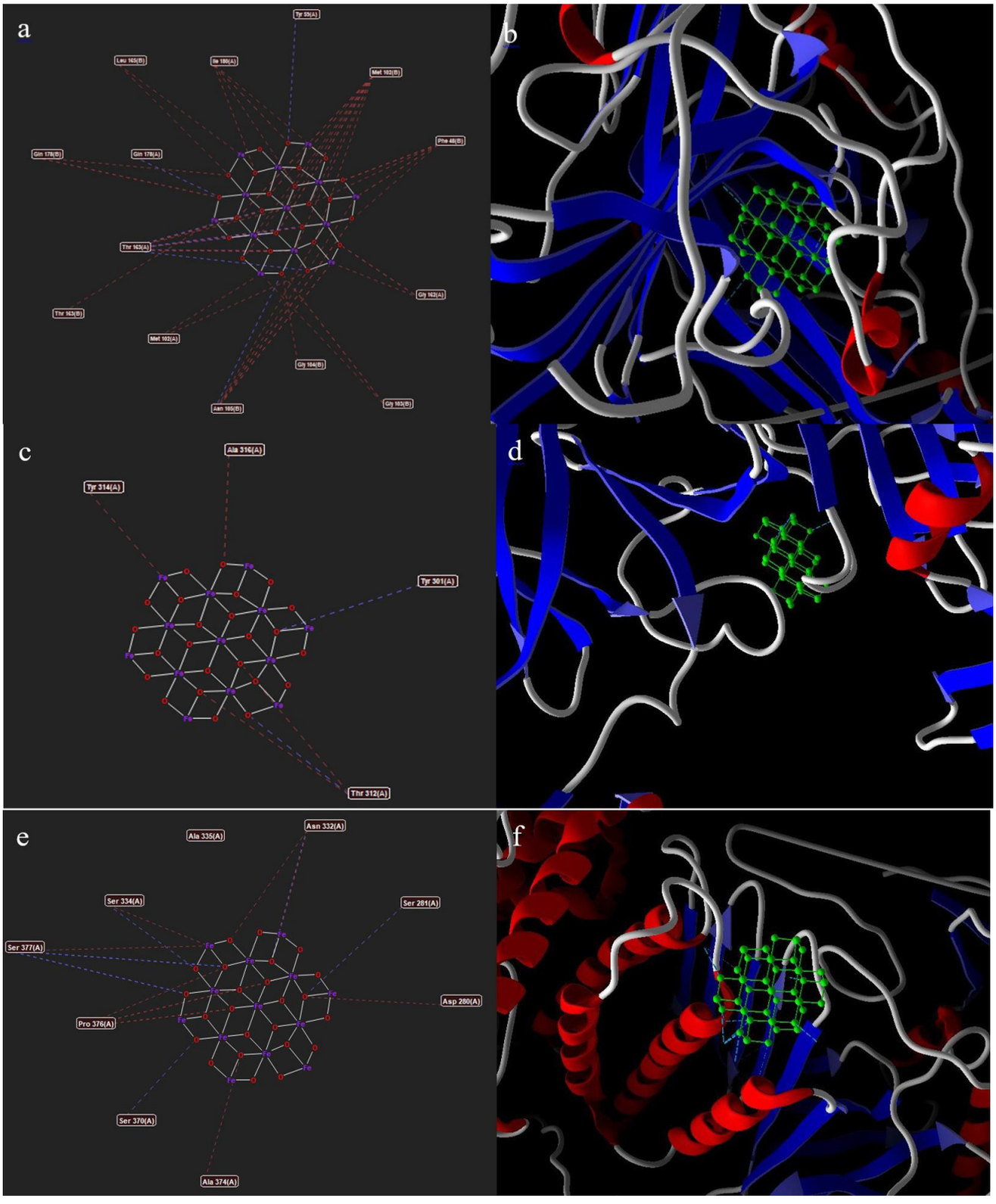


**Fig. 7.** a, b) The interactions between FeNPs and the amino acids of the HSV-1 gD. c, d) The interactions between CuNPs and the amino acids of the HSV-1 gB. e, f) The interactions between CuNPs and the amino acids of the HSV-1 gH/gL. Hydrogen bonds and steric interactions are shown as blue and red lines, respectively.

are responsible for viral initial attachment to the host cell (3). Viral envelope gB mediates the initial attachment by interacting with heparan sulfate proteoglycans (HS GP). Following the conformational changes, gD interacts with one of three potential entry receptors, namely, herpes virus entry mediator, a member of the tumor necrosis factor receptor family; Nectin-1, a member of the immunoglobulin superfamily; and 3-O sulfated HS (3-OS-HS), a member of HS family. gB, gH, and gL facilitate the binding of gD to the cell receptors and the fusion process (12). Molecular docking studies were conducted to recognize and apprehend the interaction and binding affinity of NPs with HSV-1 glycoproteins. According to the result of docking studies, the antiviral activity of synthesized CuNPs and FeNPs can stem from the blockage of the entry process of the virus because of the interaction with viral envelope glycoproteins.

Results of this study showed the considerable antiviral potential of the combination of CuNPs and FeNPs against HSV-1 under the synergism mechanism. In addition, the antiviral effect of FeNPs against HSV-1 was investigated to examine whether FeNPs were involved in the antiviral activity when they were utilized to adsorb CuNPs. Results demonstrated that treating HSV-1 with only FeNPs resulted in reductions in virus titers. Hence, they can provide a novel insight towards the inhibiting effect on HSV-1 and rationalized their development for infection prevention.

Studies have approved the fact that NPs were effective as antiviral agents against HSV-1. Szymańska et al. reported that silver nanoparticles (AgNPs) prevented HSV-1 attachment and penetration which is in agreement with the findings of our docking results. They suggested that HSV-1 inactivation might be caused by a direct interaction between NPs and viral glycoproteins. The results indicated that NPs can interact with a proline-rich region of HSV-1 gD and consequently inhibit viral penetration (23). Furthermore, Haggag et al. investigated the antiviral potential of biosynthesized AgNPs against HSV-1 infection. The results showed that AgNPs had antiviral activities against HSV-1 infection. Their docking studies confirmed that the antiviral activity of AgNPs may be related to the blockage of the penetration process of the virus because of the interaction with HSV-1 glycoproteins (24).

Several limited studies were conducted to investigate the antiviral potential of CuNPs and FeNPs against viruses. Fujimori et al. examined the antiviral activity of copper (I) iodide nanoparticles (CuINPs) against an influenza A virus of swine origin (H1N1). They reported the dose-dependent antiviral activity of CuINPs on virus titer. According to their investigation, CuINPs inactivate H1N1 due to the interaction with viral proteins such as hemagglutinin and neuraminidase (25). In another study, Shionoiri et al. investigated the antiviral capacity of CuINPs against the non-enveloped virus Feline calicivirus (FCV) as a surrogate for human norovirus on Crandell-Rees feline kidney (CRFK) cells. Their data demonstrated that CuINPs reduced the infectivity of FCV to CRFK cells significantly. They suggested that CuINPs lead to the production of ROS, and subsequent oxidation of viral capsid proteins (26). Tavakoli and Hashemzadeh investigated the inhibitory potential of CuNPs against HSV-1. The results showed that CuNPs inhibited HSV-1 infectivity in a dose-dependent manner. They suggested several mechanisms to explain the CuNPs anti-HSV-1 property, including interaction with viral proteins and degradation of the viral genome (10). Choudhary et al. explained the antiviral ability of iron nanoparticles (FeNPs) against the Chikungunya virus (CHIKV) on Vero cell line. They reported a considerable reduction in viral RNA expression level, and viral titer (more than 90 %) was observed after treating the virus with FeNPs (27). Ahmed Mohamed et al. evaluated the antiviral properties of FeNPs produced by *Hyphaene thebaica* against *Poliovirus.* Their data confirmed that FeNPs inhibit *Poliovirus* particles at a concentration of 200 μg/mL – 10 μg/Ml. They also suggested interfering with FeNPs with viral attachment to host cells results in reducing *Poliovirus* infectivity (28).

## CONCLUSION

In conclusion, docking results confirmed that synthesized CuNPs and FeNPs could interact with the HSV-1 glycoproteins and interfere with viral entry. The data from this study imply that pre-treatment of HSV-1 with the combination of CuNPs and FeNPs resulted in 4.5 TCID50 reduction in viral titer. While treating HSV-1 with only FeNPs resulted in 3.25 log10 $TCID_{50}$ reductions in virus titers as compared with the virus control.

## REFERENCES


1. Gaikwad S, Ingle A, Gade A, Rai M, Falanga A, Incoronato N, et al. Antiviral activity of mycosynthesized silver nanoparticles against herpes simplex virus and human parainfluenza virus type 3. *Int J Nanomedicine* 2013; 8: 4303-4314.
2. Halder A, Das S, Ojha D, Chattopadhyay D, Mukherjee A. Highly monodispersed gold nanoparticles synthesis and inhibition of herpes simplex virus infections. *Mater Sci Eng C Mater Biol Appl* 2018; 89: 413-421.
3. Reske A, Pollara G, Krummenacher C, Chain BM, Katz DR. Understanding HSV-1 entry glycoproteins. *Rev Med Virol* 2007; 17: 205-515.
4. Trigilio J, Antoine TE, Paulowicz I, Mishra YK, Adelung R, Shukla D. Tin oxide nanowires suppress herpes simplex virus-1 entry and cell-to-cell membrane fusion. *PLoS One* 2012; 7(10): e48147.
5. Duarte LF, Farías MA, Álvarez DM, Bueno SM, Riedel CA, González PA. Herpes simplex virus type 1 infection of the central nervous system: insights into proposed interrelationships with neurodegenerative disorders. *Front Cell Neurosc*i 2019; 13: 46.
6. Ohtsu Y, Susaki Y, Noguchi K. Absorption, distribution, metabolism, and excretion of the novel Helicase-Primase inhibitor, Amenamevir (ASP2151), in Rodents. *Eur J Drug Metab Pharmacokinet* 2018; 43: 693-706.
7. Pires de Mello CP, Bloom DC, Paixão IC. Herpes simplex virus type-1: replication, latency, reactivation and its antiviral targets. *Antivir Ther* 2016; 21: 277-286.
8. Hassan H, Bello RO, Adam SK, Alias E, Meor Mohd Affandi MMR, Shamsuddin AF, et al. Acyclovir-loaded solid lipid nanoparticles: optimization, characterization and evaluation of its Pharmacokinetic profile. *Nanomaterials (Basel)* 2020; 10: 1785.
9. Rai M, Deshmukh SD, Ingle AP, Gupta IR, Galdiero M, Galdiero S. Metal nanoparticles: The protective nanoshield against virus infection. *Crit Rev Microbiol* 2016; 42: 46-56.
10. Tavakoli A, Hashemzadeh MS. Inhibition of herpes simplex virus type 1 by copper oxide nanoparticles. *J Virol Methods* 2020; 275: 113688.
11. Jeyaraj M, Gurunathan S, Qasim M, Kang M-H, Kim J-H. A comprehensive review on the synthesis, characterization, and biomedical application of platinum nanoparticles. *Nanomaterials (Basel*) 2019; 9: 1719.
12. Azizi S, Namvar F, Mahdavi M, Ahmad MB, Mohamad R. Biosynthesis of silver nanoparticles using brown marine Macroalga, *Sargassum Muticum* aqueous extract. *Materials (Basel)* 2013; 6: 5942-5950.
13. Tavakoli A, Ataei-Pirkooh A, Mm Sadeghi G, Bokharaei-Salim F, Sahrapour P, Kiani SJ, et al. Polyethylene glycol-coated zinc oxide nanoparticle: an efficient nanoweapon to fight against herpes simplex virus type 1. *Nanomedicine (Lond)* 2018; 13: 2675-2690.
14. Ayadi Hassan S, Ghadam P, Abdi Ali A. One step green synthesis of Cu nanoparticles by the aqueous extract of Juglans regia green husk: assessing its physicochemical, environmental and biological activities. *Bioprocess Biosyst Eng* 2022; 45: 605-618.
15. Ayadi Hassan S, Gorji V, Ghadam P. "The efficient magnetic separation of the four biogenic nanoparticles from aqueous media by the unmodified iron oxide nanoparticles". *Int J Environ Sci Technol* 2021; 18: 3883-3894.
16. Singh J, Kumar V, Kim K-H, Rawat M. Biogenic synthesis of copper oxide nanoparticles using plant extract and its prodigious potential for photocatalytic degradation of dyes. *Environ Res* 2019; 177: 108569.
17. Baram-Pinto D, Shukla S, Gedanken A, Sarid R. Inhibition of HSV-1 attachment, entry, and cell-to-cell spread by functionalized multivalent gold nanoparticles. *Small* 2010; 6: 1044-1050.
18. Vincent M, Duval RE, Hartemann P, Engels-Deutsch M. Contact killing and antimicrobial properties of copper. *J Appl Microbiol* 2018; 124: 1032-1046.
19. Aallaei M, Molaakbari E, Mostafavi P, Salarizadeh N, Maleksah RE, Afzali D. Investigation of Cu metal nanoparticles with different morphologies to inhibit SARS-CoV-2 main protease and spike glycoprotein using Molecular Docking and Dynamics Simulation. *J Mol Struct* 2022; 1253: 132301.
20. El-Sheekh MM, Shabaan MT, Hassan L, Morsi HH. Antiviral activity of algae biosynthesized silver and gold nanoparticles against Herps Simplex (HSV-1) virus *in vitro* using cell-line culture technique. *Int J Environ Health Res* 2022; 32: 616-627.
21. Sivaraj R, Rahman PK, Rajiv P, Salam HA, Venckatesh R. Biogenic copper oxide nanoparticles synthesis using Tabernaemontana divaricate leaf extract and its antibacterial activity against urinary tract pathogen. *Spectrochim Acta A Mol Biomol Spectrosc* 2014; 133: 178-181.
22. Abo-Zeid Y, Ismail NSM, McLean GR, Hamdy NM. A molecular docking study repurposes FDA approved iron oxide nanoparticles to treat and control COVID-19 infection. *Eur J Pharm Sci* 2020; 153: 105465.
23. Szymańska E, Orłowski P, Winnicka K, Tomaszewska E, Bąska P, Celichowski G, et al. Multifunctional Tannic Acid/Silver Nanoparticle-Based Mucoadhesive Hydrogel for Improved Local Treatment of HSV Infection: *in vitro* and *in vivo* Studies. *Int J Mol Sci* 2018; 19: 387.
24. Haggag EG, Elshamy AM, Rabeh MA, Gabr NM, Salem M, Youssif KA, et al. Antiviral potential of green synthesized silver nanoparticles of Lampranthus coccineus and Malephora lutea. *Int J Nanomedicine* 2019; 14: 6217-6229.
25. Fujimori Y, Sato T, Hayata T, Nagao T, Nakayama M,

Nakayama T, et al. Novel antiviral characteristics of nanosized copper(I) iodide particles showing inactivation activity against 2009 pandemic H1N1 influenza virus. *Appl Environ Microbiol* 2012; 78: 951-955.

26. Shionoiri N, Sato T, Fujimori Y, Nakayama T, Nemoto M, Matsunaga T, et al. Investigation of the antiviral properties of copper iodide nanoparticles against feline calicivirus. *J Biosci Bioeng* 2012; 113: 580-586.
27. Choudhary S, Kumar R, Dalal U, Tomar S, Reddy SN. Green synthesis of nanometal impregnated biomass - antiviral potential. *Mater Sci Eng C Mater Biol Appl* 2020; 112: 110934.
28. Mohamed HEA, Afridi S, Khalil AT, Ali M, Zohra T, Salman M, et al. Bio-redox potential of Hyphaene thebaica in bio-fabrication of ultrafine maghemite phase iron oxide nanoparticles ($Fe_2O_3$ NPs) for therapeutic applications. *Mater Sci Eng C Mater Biol Appl* 2020; 112: 110890.